

Supramolecular Assembly

International Edition: DOI: 10.1002/anie.201700011
German Edition: DOI: 10.1002/ange.201700011

A Stimuli-Responsive Smart Lanthanide Nanocomposite for Multidimensional Optical Recording and Encryption

Xiang Li, Yujie Xie, Bo Song, Hao-Li Zhang, Hao Chen, Huijuan Cai, Weisheng Liu, and Yu Tang*

Abstract: A stimuli-responsive lanthanide-based smart nanocomposite has been fabricated by supramolecular assembly and applied as an active material in multidimensional memory materials. Conjugation of the lanthanide complexes with carbon dots provides a stimuli response that is based on the modulation of the energy level of the ligand and affords microsecond-to-nanosecond fluorescence lifetimes, giving rise to intriguing memory performance in the spatial and temporal dimension. The present study points to a new direction for the future development of multidimensional memory materials based on inorganic–organic hybrid nanosystems.

As information science rapidly develops, memory devices with high density, security, and storage ability are urgently required and have attracted tremendous interest.^[1] One approach to increase the data security and storage density of such devices is to use stimuli-responsive fluorescent materials^[2] that can rapidly switch between different states as optical data recording and document encryption systems.^[3] Furthermore, the temporal dimension of fluorescence signals can also be introduced in optical multiplexing, which opens more opportunities to improve data storage and security.^[4] We envisioned that the synergistic use of fluorescence color and lifetime as coding elements will provide a new approach to enhance document security against forgery and increase data storage density. In a proof-of-concept study, we herein report an inorganic–organic hybrid nanosystem that enables coding in both the spatial and temporal dimension by manipulating the stimuli-responsive luminescence colors and decay lifetimes of the individual components.

Our smart nanocomposite is based on the conjugation of two different fluorophores, carbon dots and lanthanide

complexes, by supramolecular assembly, which facilitates multidimensional optical recording and encryption. On the one hand, fluorescent carbon dots (CDs) are promising carbon-based nanomaterials that have found applications in chemical sensing and bioimaging owing to their high stability, abundant surface functional groups, and environmentally friendly preparation.^[5] On the other hand, lanthanide complexes with long lifetimes, line-like emissions, and flexible coordination modes exhibit distinct advantages in the assembly of smart luminescent materials.^[6] In our design (Figure 1),

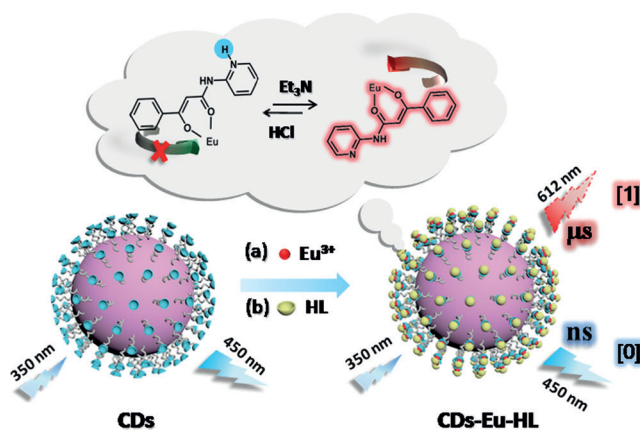


Figure 1. Operating principle of the stimuli-responsive CDs-Eu-HL nanocomposite for multidimensional optical recording and encryption.

lanthanide complexes, Eu–HL, were assembled on the surface of CDs by coordination to give a hybrid nanosystem, CDs-Eu-HL, in which the Eu^{3+} and CD species emit with microsecond-to-nanosecond lifetimes, allowing for time-resolved readout. Meanwhile, the energy levels of the ligand HL can be modulated with $\text{Et}_3\text{N}/\text{HCl}$ vapor, providing a chemical response to realize secure optical data recording. Moreover, considering the preparation of environmentally friendly aqueous fluorescent ink, which can be used in optical recording and encryption, the water solubility of the Eu^{3+} complex can be anticipated to be improved by conjugation with the water-soluble CDs.^[7] To the best of our knowledge, this inorganic–organic hybrid nanosystem is the first example of a stimuli-responsive smart nanocomposite that simultaneously stores information in the spatial and temporal dimension in a single material. We believe that our multidimensional data storage material will provide new opportunities in data recording and security.

Herein, CDs were prepared by a microwave-assisted pyrolysis method using citric acid as the carbon source and

[*] X. Li, Y. J. Xie, Prof. H. L. Zhang, H. Chen, H. J. Cai, Prof. W. S. Liu, Prof. Y. Tang
State Key Laboratory of Applied Organic Chemistry
Key Laboratory of Nonferrous Metal Chemistry and Resources Utilization of Gansu Province
College of Chemistry and Chemical Engineering
Lanzhou University
Lanzhou 730000 (China)
E-mail: tangyu@lzu.edu.cn

Dr. B. Song
State Key Laboratory of Fine Chemicals
School of Chemistry
Dalian University of Technology
Dalian 116024 (China)

Supporting information and the ORCID identification number(s) for the author(s) of this article can be found under:
<http://dx.doi.org/10.1002/anie.201700011>.

urea as a surface-passivation agent.^[8] The chemical structure of the CDs was characterized by transmission electron microscopy (TEM), X-ray photoelectron spectroscopy (XPS), and Fourier transform infrared spectroscopy (FTIR; see the Supporting Information, Figures S1–S3). We thus confirmed the presence of abundant carboxyl and amide groups on the surface of the as-obtained CDs. These functional groups provide plenty of coordination sites that can directly chelate Eu^{3+} ions. The fluorescence spectra of the CDs reveal optimal excitation and emission wavelengths of 349 nm and 448 nm, respectively (Figure S1 d). Additionally, the CDs show excellent fluorescence stability over a broad pH range (3–11) and under continuous excitation for one hour (Figure S4).

Interestingly, the fluorescence of the CDs undergoes a significant red shift from 449 to 491 nm upon an increase in the solute concentration from 10 to 300 $\mu\text{g mL}^{-1}$ (Figure S5). The fluorescence color changes from blue to green, which is consistent with the corresponding chromaticity coordinates (Figure S6). This red shift is best attributed to re-absorption in view of the spectral overlap between absorption and emission (Figure S7), which can occur at small interparticle distances.^[9] This was further confirmed by the fact that the average lifetime of the fluorescence of the CDs changed from 9.42 to 7.72 ns as the concentration was increased (Figure S8 and Table S1) because re-absorption processes compete with radiative transitions and then shorten the lifetime.^[10] Furthermore, the significant shift in wavelength that is described above is somewhat similar to the excitation-dependent fluorescence properties of the as-obtained CDs.^[9b,c] We believe that these interesting properties of the CDs should be helpful in anti-counterfeiting. First, printing patterns can only be observed under a UV lamp when CDs are utilized as the fluorescent ink (Figure S9). Moreover, when the concentration of the CDs in the ink changes, the fluorescence color also changes. As shown in Figure S10, the part of the image printed with an ink with a low CD concentration was completely invisible in daylight unlike the area printed at a higher CD concentration, which can make anti-counterfeiting marks difficult to duplicate.

As the energy levels of the amide-type β -diketone ligand *N*-(2-pyridinyl)benzoylacetamide (HL) can be modulated by acid/base vapor,^[11] we further designed a stimuli-responsive nanocomposite that combines the advantages of the CDs and Eu^{3+} complexes by coordination effects. The Eu^{3+} ions act as bridges to join the CDs and HL ligands. The successful supramolecular assembly of Eu-HL on the surface of the CDs was investigated by FTIR, UV/Vis absorption, and XPS spectroscopy. As shown in Figure S11, the HL ligands exhibited characteristic C–H in-plane and out-of-plane bending and stretching vibrations of the pyridine group at 1157 and 908 cm^{-1} , respectively. The absorption peaks in the 1435–1547 cm^{-1} region can also be attributed to $\nu(\text{C}=\text{C})$ and $\nu(\text{C}=\text{N})$ bands of the pyridine group. Enol-type C=O stretching vibrations of the β -diketone give rise to the peak at 1652 cm^{-1} . These peaks can also be found in the spectra of CDs-Eu-HL and illustrate that Eu-HL is successfully assembled on CDs through supramolecular coordination to form the smart nanosystem. The CDs-Eu-HL composites display

the characteristic absorption bands of CDs and the Eu-HL complexes in the UV/Vis absorption spectra (Figure S12).

Furthermore, a full-scan XPS plot (Figure S13) confirmed that the CDs-Eu-HL composite was mainly composed of C, N, and O. The corresponding high-resolution C 1s, N 1s, and O 1s XPS spectra revealed the presence of carbonyl, carboxyl, and amine groups, which was also confirmed by FTIR spectroscopy. Furthermore, we also observed a weak peak corresponding to Eu 3d (Figure S13 a). The high-resolution Eu 3d XPS spectrum (Figure S14) shows two peaks, corresponding to the $3d_{5/2}$ (1134.7 eV) and $3d_{3/2}$ (1164.8 eV) states of Eu^{3+} ,^[12] which further indicated that the surface of the CDs has been successfully functionalized with Eu-HL. The Eu^{3+} content of the CDs-Eu-HL composites was determined to be 22.51 wt % by thermogravimetric analysis (TGA). Similarly, the as-obtained CDs-Eu-HL composites also display typical excitation-wavelength-dependent fluorescence owing to the presence of the CDs. As shown in Figure S15, the emission peak is gradually red-shifted from 443 to 552 nm when the excitation wavelength is increased from 340 to 500 nm.

To study the stimulus response of the nanodevice, we investigated the energy levels of the ligand HL and deprotonated ligand L^- in the Gd^{3+} complexes on the CD platform. The corresponding energy levels of the triplet excited states ($^3\pi\pi^*$) of the ligand were calculated from the low-temperature (77 K) phosphorescence spectra of the corresponding Gd^{3+} complexes in a 1:1 methanol/ethanol mixture. According to Latva's empirical rule, an optimal ligand-to-metal energy transfer process for Ln^{3+} needs $\Delta E = ^3\pi\pi^* - ^5D_1 = 2500\text{--}4000 \text{ cm}^{-1}$ for Eu^{3+} .^[13] Based on the low-temperature phosphorescence spectrum of the CDs-Gd-HL nanocomposites, we calculated the energy level of the triplet excited state of the ligand HL to be 22026 cm^{-1} , which is not very suitable for energy transfer to the 5D_0 level of Eu^{3+} (17500 cm^{-1} ; Figure S16 a). However, the energy level of the triplet excited state of HL can be tuned by deprotonation on the CDs. As shown in Figure S16 b, the corresponding energy level of the ligand L^- in the CDs-Gd-L nanocomposite (20790 cm^{-1}) was located approximately 3290 cm^{-1} above the 5D_0 level of Eu^{3+} . Thus efficient intramolecular energy transfer is possible. Not surprisingly, we observed the emissions characteristic of the Eu^{3+} ion in the fluorescence spectrum of the EuL complex, which were attributed to the $^5D_0 \rightarrow ^7F_J$ ($J=0\text{--}4$) transitions upon excitation at $\lambda_{\text{ex}} = 370 \text{ nm}$ (Figure S17).

To test potential applications of the CDs-Eu-HL nanocomposites, we further studied the fluorescence properties of the nanocomposites after deposition on filter paper (with no background UV fluorescence). The paper was first dipped into an aqueous solution of CDs-Eu-HL and then dried in air. The broad emission peak at 450 nm was attributed to the CDs, and the emission peak at 612 nm was assigned to the characteristic transitions of Eu^{3+} ions. Interestingly, the fluorescence quickly changed from blue to blue-violet upon exposure to Et_3N vapor (Figures 2 a and S18). The average bi-exponential fluorescence lifetime of Eu^{3+} in the CDs-Eu-HL is 390.4 μs (Figure 2 b and Table S2), which increases remarkably to 562.22 μs after exposure to the Et_3N vapor and decreases again to 396.62 μs upon exposure to HCl gas. Good reversibility was observed even after six cycles (Figure 2 c).

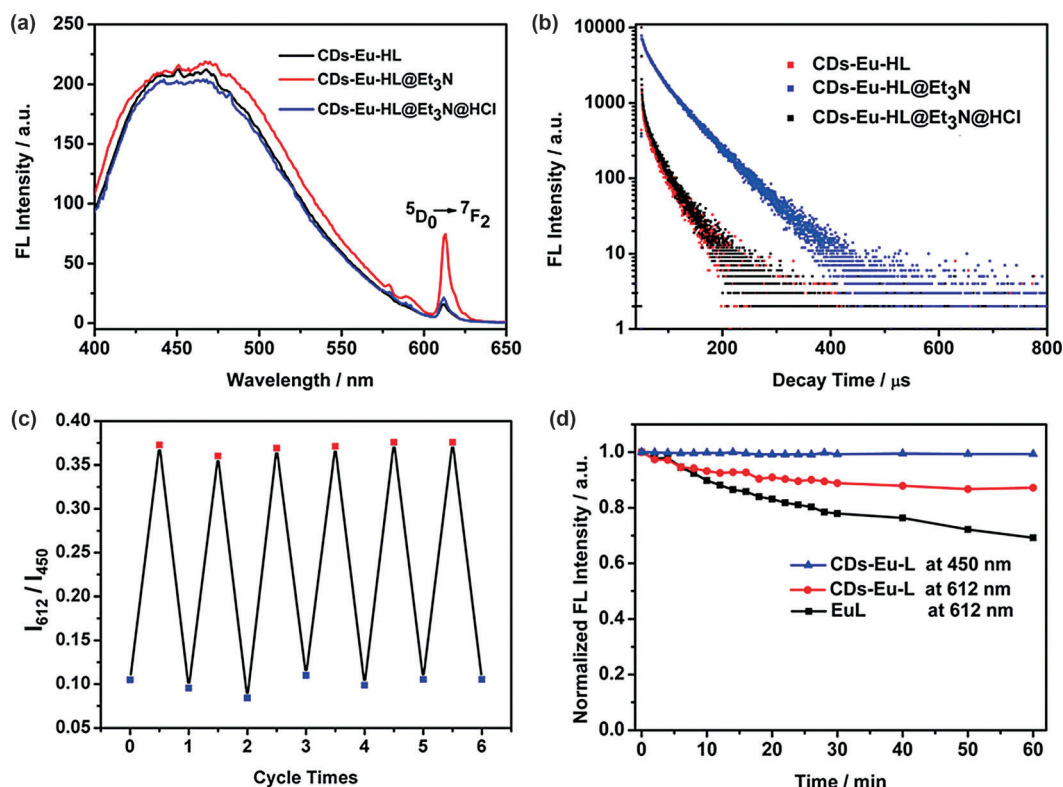


Figure 2. a) Fluorescence emission spectra and b) fluorescence lifetime decay profiles from the 5D_0 energy level of the CDs-Eu-HL nanocomposites: Changes after exposure to Et_3N vapor and HCl gas ($\lambda_{ex}=350$ nm, $\lambda_{em}=612$ nm). c) Changes in the ratio of the emission intensities at 612/450 nm of the CDs-Eu-HL nanocomposites during cycles of exposure to Et_3N /HCl vapor. d) Fluorescence intensities of the CDs-Eu-HL nanocomposites and EuL complexes on filter paper during continuous excitation with a UV beam ($\lambda_{ex}=350$ nm). Irradiation time: 0 to 60 min ($\lambda_{em}=612$ and 450 nm, respectively).

To demonstrate the performance of our hybrid nano-system as a secure memory device, the acronym of Lanzhou University (LZU) was handwritten on a filter paper with a gel pen loaded with the CDs-Eu-HL aqueous solution as fluorescent ink (Figure S18). These three letters were almost invisible in daylight. Upon irradiation with a UV lamp (365 nm), bright blue letters became visible. Upon exposure to Et_3N vapor, the fluorescence changed immediately from blue to blue-violet in 10 s. Remarkably, the blue fluorescence reappeared when the filter paper was exposed to HCl gas. Moreover, excitation-wavelength-dependent fluorescence was also observed (Figure S19). Furthermore, the photoluminescence stability of the Eu^{3+} complexes clearly improved when conjugated to the CDs (Figure 2d). Specifically, the fluorescence emission intensity of Eu^{3+} in the CDs-Eu-HL nanocomposite upon exposure to Et_3N vapor showed a slight decrease after continuous excitation for one hour (Figure 2d, red curve), whereas the fluorescence intensity of the free complex EuL at 612 nm declined more strongly (Figure 2d, black curve). In contrast, the intensity of the fluorescence emission at 450 nm of the CDs-Eu-HL nanohybrid (Figure 2d, blue curve) remained almost constant, similar to that of the original CDs (Figure S4b).

Based on the remarkable fluorescence properties of the CDs-Eu-HL nanocomposite, we next tried to expand its potential utility to multidimensional optical recording and encryption. A two-color microarray data storage pattern was

fabricated according to the binary codes of the standard 8 bit ASCII characters, with blue and blue-violet spots representing “0” and “1”, respectively. According to the ASCII binary codes, the null character is translated into “00000000” while the capital letter “L” can be translated into “01001100”. We carried out this encoding–reading experiment using a desktop inkjet printer (Canon ip2780), and solutions of the CDs-Eu-HL nanocomposite and the original CDs were used as the red and blue inks, respectively. Next, we printed patterns on filter paper substrates and then obtained fluorescence images under UV (365 nm) illumination. In this experiment, the inkjet printer acts just like an encryptor, which can be used to encode the raw information (Figure 3a). Therefore, as shown in Figure 3b, all blue fluorescent signals were collected as binary coding and can merely be translated into null characters according to the ASCII binary codes. However, after exposure to Et_3N vapor, the blue fluorescent signals that were due to the CDs-Eu-HL nanocomposite rapidly changed to blue-violet. After this “chemical decoding” step, the fluorescent dot matrix can be easily read and translated into “LZU”, the acronym of Lanzhou University. Moreover, the information can be encrypted again by exposure to HCl gas owing to the good fluorescence reversibility of the CDs-Eu-HL nanocomposite as mentioned above. Owing to these remarkable properties, the security of this binary coding system has been significantly improved to avoid information leakage.

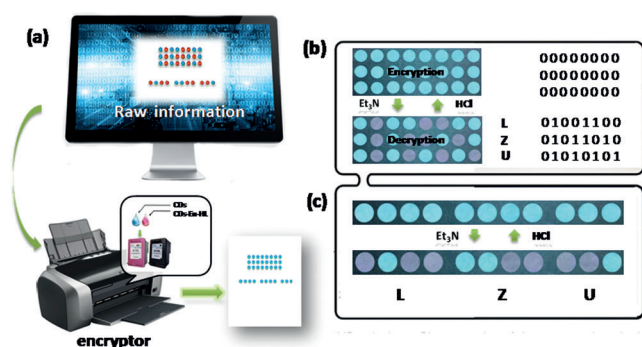


Figure 3. a) Schematic illustration of the information coding, reading, encryption, and decryption process. Digital photographs of b) binary-coded and c) Morse-coded two-color microarray data storage chips.

As an information coding standard, the Morse code has been used for longer than any other encoding program. Originally, the Morse code represents characters (including letters, numbers, and symbols) by a variety of specific combinations of short and long signals called “dots” and “dashes”. In consideration of the dual-channel fluorescence output of the CDs-Eu-HL nanocomposite, we can encrypt and transmit information by using the Morse code, in which blue and blue-violet spots represent “dashes” and “dots”, respectively. As shown in Figure 3c, we obtained raw information that had been encrypted by the inkjet printer. Initially, we only observed some blue fluorescent spots. However, after exposure to Et₃N vapor, we can easily retrieve the valuable information, which was decrypted into “LZU” according to the rules of the Morse code. The information can also be concealed again by exposure to HCl vapor.

As the fluorescence lifetime of the CDs-Eu-HL nanocomposite ranges from microseconds (Eu³⁺: 390.40 μs, Table S2) to nanoseconds (CDs: 7.78 ns, Figure S20), improvements in information security and data storage domains can be realized with a new optical coding and decoding dimension. To confirm the temporal/dimensional optical coding, time-resolved emission spectra of CDs-Eu-HL and the nanocomposite after exposure to Et₃N vapor and HCl gas were collected (Figures 4a and S21). Obvious changes in the fluorescence intensities at 450 nm and 613 nm were seen. As shown in Figure 4a, the peak at 450 nm disappeared when the delay was set to 100 μs while the peak at 613 nm gradually decreased in intensity when the delay time became much longer. Figure 4b shows a simulation diagram of lifetime-encoded document security and data storage as the oval was printed with CDs while the letters (LZU) were printed with CDs-Eu-HL. First, the blue fluorescence ascribed to the CDs can be easily observed, while the blanks show a word, namely “Chemistry”. After exposure of the pattern to Et₃N vapor, along with an extension of the delay time, the blue fluorescence of the CDs disappears, revealing the background color. At that time, the acronym of Lanzhou University, “LZU”, emerges owing to the long fluorescence lifetime of the Eu³⁺ ions (Figure 4b). This proposition was confirmed to some extent by steady-state and time-gated fluorescence images (Figure 4c). The changes in the fluorescence color are consistent with the time-resolved emission spectra.

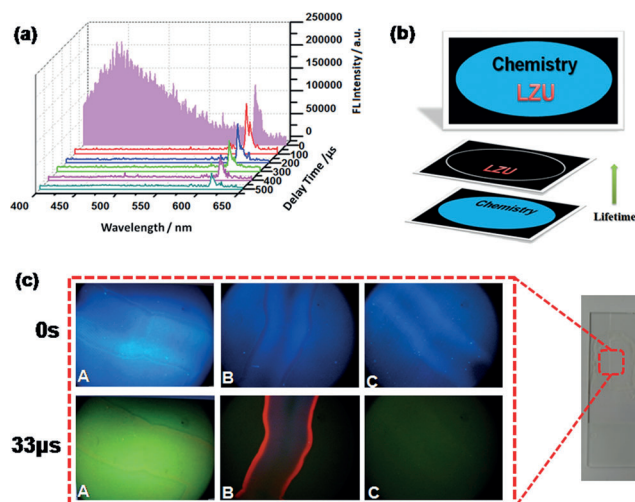


Figure 4. a) Time-resolved emission spectra of CDs-Eu-HL nanocomposites after exposure to Et₃N vapor for delay times from 0 to 500 μs. b) Simulation of the lifetime-encoded document security and data storage process. c) Steady-state and time-gated fluorescence images of a glass cover slip coated with CDs-Eu-HL and CDs (A), after exposure to Et₃N vapor (B), and after exposure to HCl gas (C). Delay time: 33 μs.

Moreover, the ⁵D₀ excited-state lifetime of Eu³⁺ was prolonged to 562.22 μs after exposure to Et₃N vapor. Thus, according to the decoding rule that we have stipulated, the authenticity and accuracy of encoded information can be validated through a further processing step. As shown in Figure S22, the encoded information (LZU) inscribed with the CDs-Eu-HL nanocomposite can only be read during 10–300 μs. Upon exposure to Et₃N vapor, LZU can also be observed during 400–600 μs. This result provides a new option for a more secure way of document encryption so that only well-trained and authorized personnel who know the correct decoding rule and thus the fluorescence decay lifetimes are able to access the confidential information.

In summary, a novel vapor-responsive lanthanide optical material (CDs-Eu-HL) has been fabricated by supramolecular assembly, and applied in a multidimensional information memory device. The smart nanocomposite showed strong and stable fluorescence as well as microsecond-to-nanosecond fluorescence lifetimes and remarkable changes in the fluorescence upon exposure to acidic or basic environments. The conjugation of CDs and Eu-HL improved not only the water solubility but also the stability of the Eu-HL photoluminescence. Optical recording and encryption in the spatial and temporal dimension was enabled by the stimuli-response energy-level modulation of the ligand and the various fluorescence lifetimes of the lanthanide ions and CDs. This work opens new opportunities for future memory devices carrying more codes through a combination of color, intensity, and lifetime, revealing the potential of luminescence as a powerful tool to deal with the challenges in high-density data storage as well as document security against forgery.

Acknowledgements

This work was financially supported by the National Natural Science Foundation of China (Projects 21471071, 21431002, 51525303, and 21233001).

Conflict of interest

The authors declare no conflict of interest.

Keywords: carbon dots · fluorescence · lanthanides · nanocomposites · stimuli-responsive materials

- [1] a) J. J. Yang, D. B. Strukov, D. R. Stewart, *Nat. Nanotechnol.* **2013**, *8*, 13; b) H. Sun, S. Liu, W. Lin, K. Zhang, W. Lv, X. Huang, F. Huo, H. Yang, G. Jenkins, Q. Zhao, W. Huang, *Nat. Commun.* **2014**, *5*, 3601–3609; c) E. Y.-H. Hong, C.-T. Poon, V. W.-W. Yam, *J. Am. Chem. Soc.* **2016**, *138*, 6368–6371; d) C. T. Poon, D. Wu, W. H. Lam, V. W.-W. Yam, *Angew. Chem. Int. Ed.* **2015**, *54*, 10569–10573; *Angew. Chem.* **2015**, *127*, 10715–10719.
- [2] a) Y. Sagara, T. Kato, *Nat. Chem.* **2009**, *1*, 605–610; b) M. Tanioka, S. Kamino, A. Muranaka, Y. Ooyama, H. Ota, Y. Shirasaki, J. Horigome, M. Ueda, M. Uchiyama, D. Sawada, S. Enomoto, *J. Am. Chem. Soc.* **2015**, *137*, 6436–6439; c) A. Kishimura, T. Yamashita, K. Yamaguchi, T. Aida, *Nat. Mater.* **2005**, *4*, 546–549; d) K. Li, Y. Xiang, X. Y. Wang, J. Li, R. R. Hu, A. J. Tong, B. Z. Tang, *J. Am. Chem. Soc.* **2014**, *136*, 1643–1649; e) T. A. Darwish, R. A. Evans, M. James, N. Malic, G. Triani, T. L. Hanley, *J. Am. Chem. Soc.* **2010**, *132*, 10748–10755; f) X. Li, H. Chen, A. M. Kirillov, Y. J. Xie, C. F. Shan, B. K. Wang, C. L. Shi, Y. Tang, *Inorg. Chem. Front.* **2016**, *3*, 1014–1020.
- [3] a) W. Wang, N. Xie, L. He, Y. Yin, *Nat. Commun.* **2014**, *5*, 5459–5465; b) K. Jiang, L. Zhang, J. Lu, C. Xu, C. Cai, H. Lin, *Angew. Chem. Int. Ed.* **2016**, *55*, 7231–7235; *Angew. Chem.* **2016**, *128*, 7347–7351; c) J. W. Chung, S. J. Yoon, S. J. Lim, B. K. An, S. Y. Park, *Angew. Chem. Int. Ed.* **2009**, *48*, 7030–7034; *Angew. Chem.* **2009**, *121*, 7164–7168; d) Y. Wu, Y. Xie, Q. Zhang, H. Tian, W. Zhu, A. Li, *Angew. Chem. Int. Ed.* **2014**, *53*, 2090–2094; *Angew. Chem.* **2014**, *126*, 2122–2126.
- [4] Y. Q. Lu, J. B. Zhao, R. Zhang, Y. J. Liu, D. M. Liu, E. M. Goldys, X. Yang, P. Xi, A. Sunna, J. Lu, Y. Shi, R. C. Leif, Y. J. Huo, J. Shen, J. A. Piper, J. P. Robinson, D. Y. Jin, *Nat. Photonics* **2014**, *8*, 32–36.
- [5] a) F. R. Baptista, S. A. Belhout, S. Giordani, S. J. Quinn, *Chem. Soc. Rev.* **2015**, *44*, 4433–4453; b) S. J. Zhu, Q. N. Meng, L. Wang, J. H. Zhang, Y. B. Song, H. Jin, K. Zhang, H. C. Sun, H. Y. Wang, B. Yang, *Angew. Chem. Int. Ed.* **2013**, *52*, 3953–3957; *Angew. Chem.* **2013**, *125*, 4045–4049; c) S. J. Zhu, Y. B. Song, J. R. Shao, X. H. Zhao, B. Yang, *Angew. Chem. Int. Ed.* **2015**, *54*, 14626–14637; *Angew. Chem.* **2015**, *127*, 14834–14846; d) X. M. Li, Y. L. Liu, X. F. Song, H. Wang, H. S. Gu, H. B. Zeng, *Angew. Chem. Int. Ed.* **2015**, *54*, 1759–1764; *Angew. Chem.* **2015**, *127*, 1779–1784; e) X. M. Li, M. C. Rui, J. Z. Song, Z. H. Shen, H. B. Zeng, *Adv. Funct. Mater.* **2015**, *25*, 4929–4947.
- [6] a) H. Dong, S. R. Du, X. Y. Zheng, G. M. Lyu, L. D. Sun, L. D. Li, P. Z. Zhang, C. Zhang, C. H. Yan, *Chem. Rev.* **2015**, *115*, 10725–10815; b) Y. Zhang, T.-T. Shen, A. M. Kirillov, W.-S. Liu, Y. Tang, *Chem. Commun.* **2016**, *52*, 7939–7942; c) T.-T. Shen, Y. Zhang, A. M. Kirillov, H.-J. Cai, K. Huang, W.-S. Liu, Y. Tang, *Chem. Commun.* **2016**, *52*, 1447–1450; d) H. Chen, Y. J. Xie, A. M. Kirillov, L. L. Liu, M. H. Yu, W. S. Liu, Y. Tang, *Chem. Commun.* **2015**, *51*, 5036–5039; e) Y. J. Xie, W. Y. Wu, H. Chen, X. Li, H. L. Zhang, L. L. Liu, X. X. Shao, C. F. Shan, W. S. Liu, Y. Tang, *Chem. Eur. J.* **2016**, *22*, 8339–8345.
- [7] C. Dian, A. Zhu, Y. Tian, *Acc. Chem. Res.* **2014**, *47*, 20–30.
- [8] a) S. N. Qu, X. Y. Wang, Q. P. Lu, X. Y. Liu, L. J. Wang, *Angew. Chem. Int. Ed.* **2012**, *51*, 12215–12218; *Angew. Chem.* **2012**, *124*, 12381–12384.
- [9] a) Y. H. Chen, M. T. Zheng, Y. Xiao, H. W. Dong, H. R. Zhang, J. L. Zhuang, H. Hu, B. F. Lei, Y. L. Liu, *Adv. Mater.* **2016**, *28*, 312–318; b) Y. Wang, S. Kalytchuk, Y. Zhang, H. C. Shi, S. V. Kershaw, A. L. Rogach, *J. Phys. Chem. Lett.* **2014**, *5*, 1412–1420; c) H. B. Zeng, G. T. Duan, Y. Li, S. K. Yang, X. X. Xu, W. P. Cai, *Adv. Funct. Mater.* **2010**, *20*, 561–572.
- [10] J. R. Lakowicz, *Principles of Fluorescence Spectroscopy*, Springer Science & Business Media, Baltimore, **2007**.
- [11] J. Xu, L. Jia, N. Z. Jin, Y. F. Ma, X. Liu, W. Y. Wu, W. S. Liu, Y. Tang, F. Zhou, *Chem. Eur. J.* **2013**, *19*, 4556–4562.
- [12] a) X. L. Tan, X. K. Wang, H. Geckeis, TH. Rabung, *Environ. Sci. Technol.* **2008**, *42*, 6532–6537; b) X. Tan, Q. H. Fan, X. K. Wang, B. Grambow, *Environ. Sci. Technol.* **2009**, *43*, 3115–3121.
- [13] a) M. Latva, H. Takalo, V. M. Mikkala, C. Matachescu, J. C. Rodriguez-Ubis, J. Kankare, *J. Lumin.* **1997**, *75*, 149–169; b) Y. S. Zhou, X. M. Li, L. J. Zhang, Y. Guo, Z. H. Shi, *Inorg. Chem.* **2014**, *53*, 3362–3370.

Manuscript received: January 1, 2017

Revised: January 15, 2017

Final Article published: ■ ■ ■ ■ ■ ■ ■ ■ ■ ■

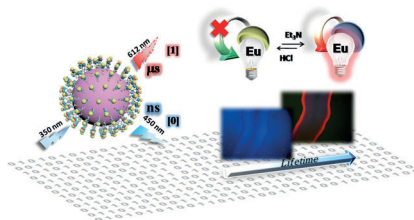
Communications



Supramolecular Assembly

X. Li, Y. J. Xie, B. Song, H. L. Zhang,
H. Chen, H. J. Cai, W. S. Liu,
Y. Tang*     

A Stimuli-Responsive Smart Lanthanide
Nanocomposite for Multidimensional
Optical Recording and Encryption



Hidden talents: A stimuli-responsive lanthanide nanocomposite was fabricated by functionalization of carbon dots with lanthanide complexes and applied in a multidimensional memory device. The fluorescence lifetime and color can be changed by modulating the energy levels of the lanthanide ligand.